A Novel Negative Dielectric Constant Material Based on Phosphoric Acid Doped Poly(benzimidazole)

Keith L. Gordon,[1] Jin Ho Kang,[2] Cheol Park,[2,3] Peter T. Lillehei,[1] Joycelyn S. Harrison[1]

[1]*Advanced Materials and Processing Branch, NASA-Langley Research Center, Hampton, Virginia 23681-2199*
[2]*National Institute of Aerospace, Hampton, Virginia 23666*
[3]*Department of Mechanical and Aerospace Engineering, University of Virginia, Charlottesville, Virginia 22904-4746*

Received 23 February 2011; accepted 5 May 2011
DOI 10.1002/app.36248
Published online 1 February 2012 in Wiley Online Library (wileyonlinelibrary.com).

ABSTRACT: Metamaterials or artificial negative index materials (NIMs) have generated great attention because of their unique electromagnetic properties. The main challenge in current NIM development is creating a homogenous NIM without the need of complex geometric architectures consisting of capacitors and inductors or aggregated fillers, but possessing a tunable plasma frequency. A natural material that can exhibit negative values for permittivity and permeability simultaneously has not been found, or discovered. If one can design a negative dielectric constant material with a tunable plasma frequency of interest, implementing negative permeability into the material or system would be much more readily achievable to create a metamaterial. In this regard, a novel negative dielectric constant material, which is an essential key to creating the NIMs, was developed by doping ions into a polymer, a protonated poly(benzimidazole) (PBI). The doped PBI showed a negative dielectric constant at frequencies of kHz to MHz because of its reduced plasma frequency and an induction effect. As temperature increased, the dielectric spectrum changed from a relaxation to a resonance behavior and exhibited a larger magnitude of negative dielectric constant at a lower frequency. The conductivity of the doped PBI measured as a function of both temperature and frequency followed the same trend as the dielectric constant. With respect to the dielectric constant and the conductivity data, it can be assumed that the origin of the negative dielectric constant is attributed to the resonance behavior of the highly mobile ions at elevated temperatures and high frequencies. © 2012 Wiley Periodicals, Inc. J Appl Polym Sci 125: 2977–2985, 2012

Key words: high performance polymers; polymer synthesis and characterization; dielectric properties; metamaterials; resonance frequency

INTRODUCTION

Metamaterials or artificial Negative Index Materials (NIMs) are a new class of electromagnetic (EM) materials that have generated great attention over the last 10 years due to their unique electromagnetic (EM) properties.[1–5] Through the confirmed existence of negative refraction in resonant radio frequency (RF) structures with negative permittivity and permeability yield, researchers with DOD and quite recently NASA are exploring many exciting applications for these materials, such as lightweight, compact RF or microwave structures, as improved optics for imaging systems, wireless antenna suits, reduction of energy/power beam dispersion, and also as EM cloaking devices, in which the material is used to render a volume effectively invisible to incident radiation.[6,7] NIMs are constructed with specially designed architecture and inclusions and exhibit a negative index of refraction, which is a property not found in any known naturally occurring material. The property of a metamaterial can be described by two effective parameters: electric permittivity (ε_{eff}) and magnetic permeability (μ_{eff}). Most dielectrics only have positive permittivities, $\varepsilon > 0$. Metals will exhibit negative permittivity, $\varepsilon < 0$ at optical frequencies, and plasmas exhibit negative permittivity values in certain frequency bands.[8] A natural material that can exhibit negative values for permittivity and permeability simultaneously has not been found, nor discovered. If one can design a negative dielectric constant material with a tunable plasma frequency of interest, implementing negative permeability into the material or system would be much more readily achievable to create a metamaterial.

To date, to achieve a negative dielectric constant, two main approaches have been employed.[4,9] One approach involves the use of either a periodic structure, whose frequency spectrum simulates the response of high pass filter,[10–12] or a waveguiding structure such as a hollow metallic waveguide.[13] Under this condition, EM waves are evanescent at low frequencies and this evanescence in the small frequency gap is described in terms of negative permittivity values below some specific frequency: the corner (or cutoff) frequency. The second approach involves the use of a composite containing metal

Correspondence to: J. H. Kang (jin.h.kang@nasa.gov).

inclusions in a dielectric matrix.[4,14–16] A. N. Lagarkov verified experimentally on a micrometer level that the effective dielectric constant of a composite containing conducting microfibers (diameter = 25 μm) was negative at GHz frequencies.[14] D. P. Makhnovskiy proposed that a composite that consists of short ferromagnetic wires embedded into a dielectric matrix, can exhibit a tunable effective negative dielectric constant under a dc magnetic field.[15–18] However, the first approach involves assembling periodic geometrical structures made up of inductors and capacitors on a micrometer scale, which is extremely difficult and not readily applicable for producing commercial metamaterials with conventional materials. The second approach of using metal inclusions is hampered by the difficulty in preparing a homogenous material without aggregated fillers. The limitation of tunability of the resonance frequency is another big problem since the resonance frequency can be tuned only by dimensional change of the components in these systems. However, systems based on solid polyelectrolytes, such as poly(benzimidazole) (PBI) doped with phosphoric acid may provide a homogenous material without aggregated fillers and a material with tunability of the resonance frequency. The conductivity of these materials are easy to control with doping agents such as phosphoric acid.[19–21] Additionally, the higher effective mass of the charge carriers, ions can be an advantage in controlling the plasma frequency (ω_p). With these attractive features in mind, the feasibility of using solid polyelectrolyes, as a negative effective dielectric constant material, essential for making a negative refractive index material was studied. Herein, we report a simple approach to create a homogenous NIM without aggregated fillers and with a tunable plasma frequency. PBI is synthesized and doped with phosphoric acid at various concentration levels. The techniques of infrared (IR) spectroscopy, dynamic mechanical analysis, tensile tester, and impedance analysis were used to characterize the material properties of undoped and doped PBI thin films. A Colpitts oscillator circuit was employed as a dynamic test for doped membranes. Novel temperature dependent-negative dielectric phenomena observed in a protonated PBI and a proposed mechanism for the negative dielectric constant found in the kHz range are reported. To the best of our knowledge, this is the first example of a solid polyelectrolyte displaying negative effective dielectric constant, essential for making a metamaterial.

EXPERIMENT

Synthesis of phosphoric acid doped PBI

3,3′-Diaminobenzidine (DAB), isophthalic acid (IPA), poly(phosphoric acid) (PPA), and N,N′-dimethylacetamide (DMAc) were purchased from Sigma-Aldrich chemical company and used as received. Other chemicals used were purchased from Fisher Scientific Company.

PBI was prepared using a modification of previously reported synthesis (Fig. 1).[22,23] The general process of the solution polycondensation reaction is as follows. PPA was added to a 250 mL three-necked flask equipped with a mechanical stirrer, a nitrogen inlet, and outlet. The flask was immersed in an oil bath and stirred at 80°C for several hours to remove residual air from the flask. The temperature of the PPA was taken to 140°C and a stoichiometric ratio mixture of DAB and IPA was charged into the flask under nitrogen flow while stirring. The reaction mixture was vigorously stirred at ca. 140°C for 5 h and about 200°C for 18 h. The hot slurry solution was poured into water for precipitation and the precipitated polymer was immersed in about 5 wt % Na_2CO_3 aqueous solution for at least 24 h. The polymer was obtained by vacuum filtration, washed with deionized water, and dried in a vacuum oven at about 110°C overnight.

The PBI films were prepared from 5% (w/v) solutions in DMAc. The filtered polymer solutions in DMAc were heated with vigorous stirring for several hours to facilitate dissolution of PBI. The polymer solutions were poured onto glass plates and were placed in a dry box for about 48 h to form membranes. The membranes were oven dried at about 100°C for 1 h and about 200°C for 1 h. The films were isolated from the glass plates in cold water. The PBI membrane was then dried at about 100°C for 24 h under vacuum. Acid-doped PBI film was obtained by immersing the membrane in various concentrations of aqueous phosphoric acid (50 and 60 wt %) solution for about 48 h at room temperature. The doped polymer membrane was blot dried with a paper towel and placed in an oven at about 40°C for 24–48 h under vacuum. After the membrane was dried, it was weighed to determine the amount of phosphoric acid uptake. The final weights of the doped polymer membranes after uptake increased on average by about 120%. The doping level of the membranes is determined by the concentration of phosphoric acid and the reported doping level of a PBI membrane immersed into a 60 wt % phosphoric acid solution for about 48 h was as high as five phosphoric acid molecules per repeat unit.[24]

Sample characterization

IR spectra were taken from thin films in transmission mode with a Thermoelectron IR300 spectrometer in the 4400–500 cm^{-1} range using an attenuating total reflectance-sampling accessory. AC conductivities (σ^*) and dielectric constants (ε^*) of the polymer

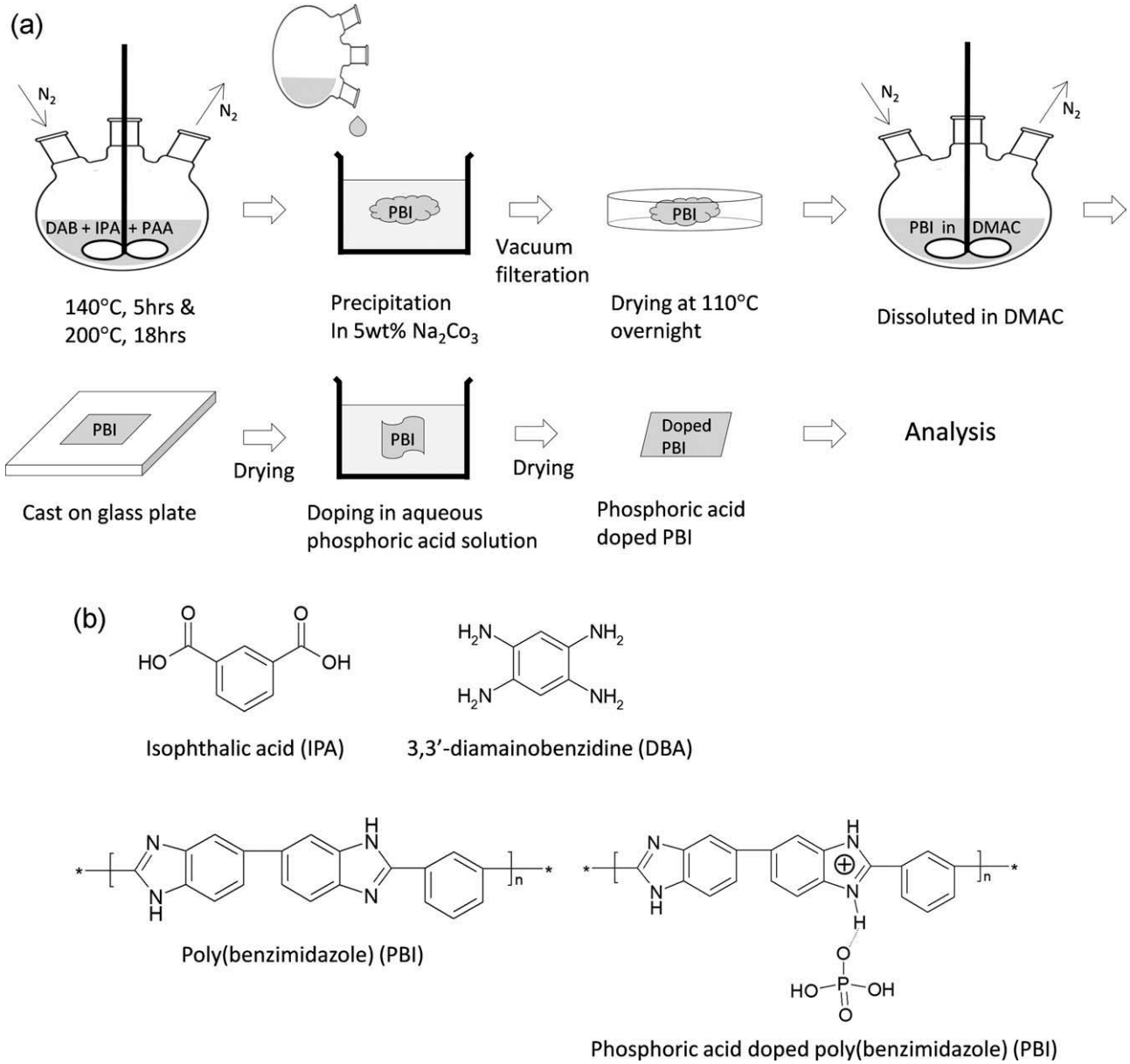

Figure 1 (a) Synthesis of phosphoric acid doped PBI and (b) chemical structures of monomers and polymers.

electrolytes were determined with an impedance (Z^*) bridge (Novocontrol system) as a function of frequency from 10 Hz to 1.53×10^6 Hz and a function of temperature from 25 ± 0.1°C to 300 ± 0.1°C by following eq. (1):

$$\varepsilon^*(\omega) = \varepsilon' - i\varepsilon'' = \frac{-i}{\omega Z^*(\omega)}\frac{1}{C_0},$$
$$\sigma^*(\omega) = \sigma' - i\sigma'' = i2\pi f\varepsilon_0(\varepsilon^* - 1) \quad (1)$$

where C_0 and ε_0 are the capacity of the empty sample capacitor and free space permittivity, respectively. Gold electrodes were deposited on both sides of the membranes after complete drying. Disk shaped films (ca. 25.4 mm-diameter, ~ 50 μm-thick) were employed for these measurements. Glass transition temperatures (T_g) was measured by a dynamic mechanical analyzer (DMA, TA Instrument DMA Q800) and determined from tan δ peaks of DMA data measured at 1 Hz. Mechanical properties of undoped and doped PBI measured by a tensile tester.

RESULTS AND DISCUSSION

IR spectra of pure PBI and doped PBI are shown in Figure 2. The interactions between PBI membranes and phosphoric acid have been extensively studied by Infrared Spectroscopy.[24,25] For PBI, a broad peak corresponding to the free N—H stretch and the self-associated, hydrogen bonded N—H groups are observed in the spectral region 4000–2500 cm^{-1} and

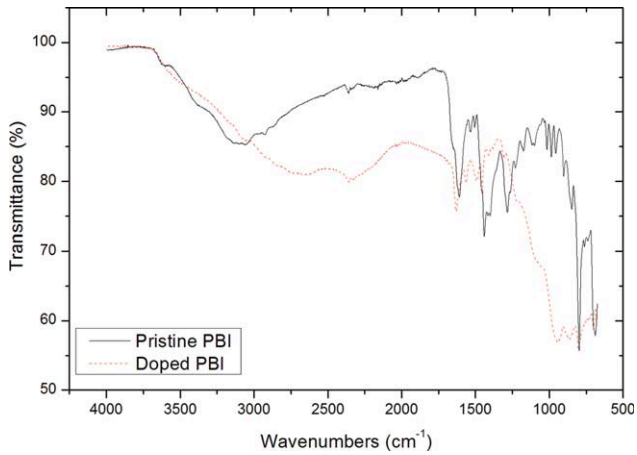

Figure 2 IR spectra of pure PBI and doped PBI. [Color figure can be viewed in the online issue, which is available at wileyonlinelibrary.com.]

are in agreement with the results in literature.[20–22] The absence of a carbonyl peak in the spectral region 1540–1870 cm^{-1} confirms ring closure. Also, the C=C and C=N stretching vibrations are observed at 1606 cm^{-1}, in-plane heterocyclic ring vibrations are observed at 1444 cm^{-1}, a breathing imidazole ring stretch is observed at 1287 cm^{-1} , and a strong absorption for out of plane C—H bending for benzene rings is observed at 799 cm^{-1}. All of which are conclusive for benzimidazoles. For H_3PO_4 doped PBI films, the IR spectrum of the PBI is greatly modified after protonation and complexation with phosphoric acid. The broad band in the 2000–3500 cm^{-1} is the result of the presence of protonated PBI, the complexation with phosphoric acid, and the existence of strong hydrogen bonding. H_3PO_4 protonates benzimidazole rings, resulting in the formation of anions (Fig. 1). As reported by Bouchet and Siebert, absorption bands in the 500–1300 cm^{-1} spectral region are characteristic of anions.[24] $H_2PO_4^-$ is the predominant anion in the entire concentration range. The $H_2PO_4^-$ anions in the membrane play a dominant role in the proton conductivity because they contain both proton acceptor and donor sites, allowing them to contribute to the overall proton transport in the system.[26] Figure 3 is a schematic representation proposed by Savinell and coworkers depicting the different mechanisms of conductivity with respect to proton migration in acid doped PBI systems. In Figure 3(b), H_3PO_4 protonates the nitrogen atom of the imino group of the PBI matrix and proton migration occurs between protonated and nonprotonated imino nitrogen groups on neighboring polymer chains. The protonation of PBI produces anions of H_3PO_4, which are immobilized within the PBI matrix by strong hydrogen bonding to provide a network for proton transport. In Figure 3(c), proton transfer along acid-PBI-acid is described. When the maximum degree of protonation is reached, there is an excess of H_3PO_4 within the membrane. Proton conductivity in acid doped PBI at this point would be the result of transfer of proton along acid-PBI-acid. In Figure 3(d), proton transfer mainly along the acid is depicted. With increasing acid doping level, there is more excess H_3PO_4 present within the membrane. The proton migration will primarily occur along the mixed $H_2PO_4^-...H_3PO_4$ and $N—H+...H_2PO_4^-$ anionic chains. In Figure 3(e), proton migration along acid and water is depicted. The increased addition of H_3PO_4 results in more excess acid in the polymer matrix. Proton migration will occur mainly along acid-PBI-acid or the acid and H_2O chain depending on the amount of water present within the membrane. The anions of phosphoric acid are proposed to be immobilized and held by the PBI matrix by strong hydrogen bonding thus forming a network for proton transport.[23,24,26]

Table I shows glass transition temperatures (T_g) measured by a DMA and mechanical properties of undoped and doped PBI measured by a tensile tester. Glass transition temperature, modulus, and stress at break decreased with increasing of dopant concentration because of plasticizing effect of the dopant. Elongation at break increased with increasing of dopant concentration.

Figure 4(a) shows a series of dielectric spectra of the 50% doped PBI at various temperatures as a function of frequency. The dielectric constant decreased with increasing frequency. When the sample was measured at 25 ± 0.1°C, the dielectric constant was 118 ± 0.1 at 10 Hz and decreased to 7.65 ± 0.008 at 1×10^6 Hz. When the dielectric constant was measured at elevated temperatures, the dielectric constant increased with increasing temperature. The dielectric constant measured at 10 Hz and 300 ± 0.1°C was five orders of magnitude higher than that measured at 10 Hz and 25 ± 0.1°C. Most interestingly, the dielectric constant "resonance" spectrum appeared in the range of about 1×10^5 and 1×10^6 Hz. It exhibits a transition from positive to negative values, reaching a minimum at around 2×10^5 Hz [inset of Fig. 4(a)].

The increase in the dielectric constant at a low frequency is indicative of the presence of interfacial polarization. This leads to field distortion and gives rise to induced dipole moments. This effect is prevalent at low frequencies since the dipole relaxation time of this type of polarization is large. In this system, there is an abundance of mobile ions present, which results in significant interfacial polarization. The increase of the dielectric constant at lower frequencies with increasing temperatures can be explained by the higher polarization resulting from the higher mobility of doped ions at higher temperatures.

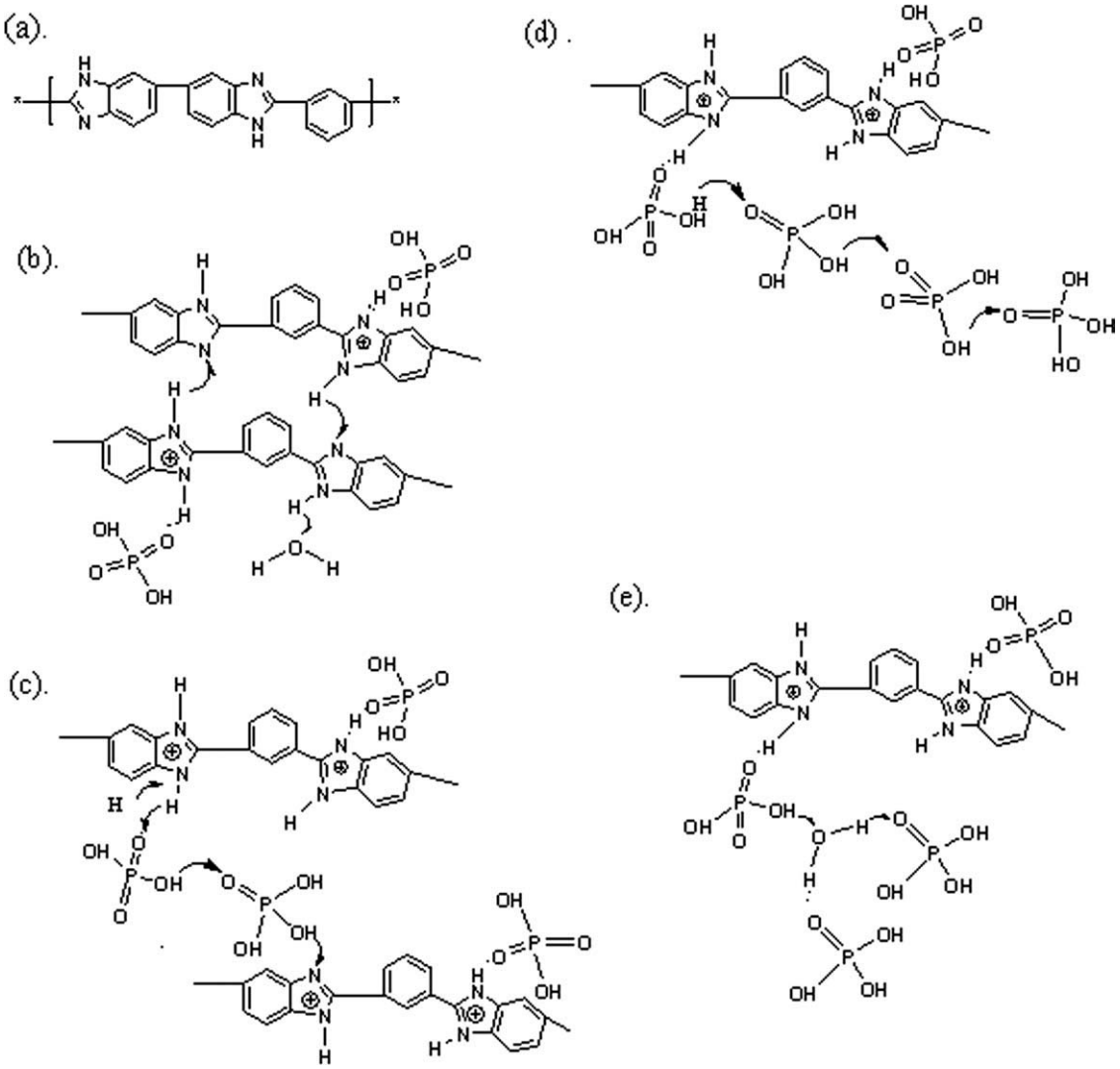

Figure 3 Schematic representation of different mechanisms of ion (proton) transport (a) PBI, (b) H_3PO_4 protonated PBI, (c) proton transfer along acid-PBI-acid, (d) proton transfer along acid, and (e) proton transfer along acid-H_2O.

To find a clear transition of a resonance behavior, the minimum dielectric constant and the frequency at the minimum (f_{min}), just above the resonance frequency (f_{res}) were recorded at each temperature and plotted in a three-dimensional (3D) space [shown as black solid squared in Fig. 4(b)]. The 3D data was projected onto each plane. The projected graphs at each plane help to understand the resonance behavior among dielectric constant, temperature and frequency. From the projected data on the dielectric constant-temperature plane (green triangles in the graph), it is shown that the minimum dielectric constant slightly increased from 7.65 ± 0.008 to 19.1 ± 0.02 over the temperature range of 25 ± 0.1°C to 120 ± 0.1°C. Above 130 ± 0.1°C, the minimum dielectric constant began to decrease gradually and reached a negative value of −124 ± 0.1 at a temperature of 160 ± 0.1°C. Above 160 ± 0.1°C, the minimum dielectric

TABLE I
Thermal and Mechanical Properties of Undoped and Doped PBI

	Glass transition temperature[a] (°C)	Modulus (GPa)	Stress at break (MPa)	Elongation at break (%)
Undoped PBI	346.66	4.59 ± 0.43	125.27 ± 7.15	11.50 ± 4.36
Doped PBI-50 wt % H_3PO_4	184.49	1.89 ± 0.16	58.13 ± 2.99	14.60 ± 1.15
Doped PBI-60 wt % H_3PO_4	165.74	0.725 ± 0.01	21.31 ± 5.22	23.01 ± 5.52

[a] Glass transition temperatures were determined from tan δ peaks of dynamic mechanical analysis (DMA) data measured at 1 Hz.

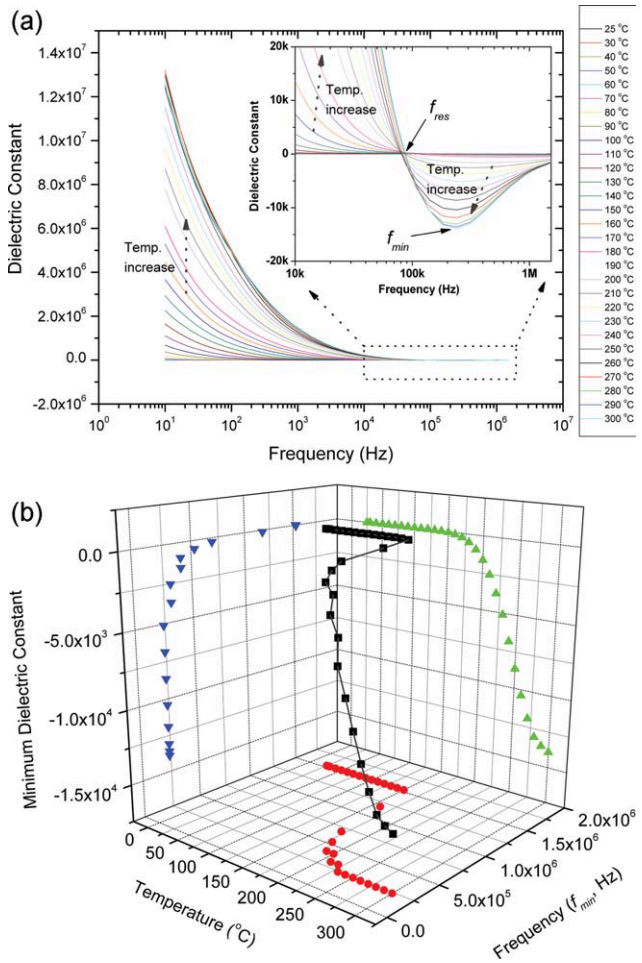

Figure 4 (a) Dielectric constant of PBI doped with 50 wt % of H_3PO_4 aqueous solution as functions of frequency and temperature and (b) 3D plot of minimum dielectric constant, temperature and frequency. [Color figure can be viewed in the online issue, which is available at wileyonlinelibrary.com.]

constant decreased steeply and reached $-0.39 \times 10^4 \pm 14$ at a temperature of 300 ± 0.1°C. The projected data on the frequency-temperature plane (red circles in the graph) clarifies the relationship between the f_{min} frequency at the minimum dielectric constant and the temperature. Over the temperature range of 25 ± 0.1°C to 150 ± 0.1°C, the f_{min} frequency remained constant because no f_{min} frequency appeared up to about 1.53×10^6 Hz, which is the highest measuring frequency limit. As the temperature increased above 160 ± 0.1°C, the f_{min} frequency decreased drastically because the mobility of the ionic charge carriers increased with increasing temperature. However, above 230 ± 0.1°C, the f_{min} frequency remains constant with increasing temperature. Finally, the projected data on the dielectric constant-frequency plane (blue inversed triangles in the graph) allows us to determine the f_{min} frequency at which the dielectric constant reaches its minimum value. Above 4×10^5 Hz, the minimum dielectric constant is relatively insensitive to frequency. Below 4×10^5 Hz, however, the dielectric constant drops dramatically over a very small frequency interval due to increased contribution of the sluggish ionic charge carriers.

The conductivity of the doped PBI was also measured as a function of frequency and temperature. The effects of frequency and temperature on the conductivity were very similar to those observed in the dielectric constant measurements as shown in Figure 5(a). The overall conductivity increased with increasing temperature, reaching a maximum at a frequency between 1×10^5 and 1×10^6 Hz. The conductivity measured at 10 Hz at a temperature of 300 ± 0.1°C was three orders of magnitude higher than that measured at 10 Hz at a temperature of 25 ± 0.1°C [Fig. 5(a)]. Above 160 ± 0.1°C, the conductivity increased very rapidly with increasing temperature and displayed a peak at a frequency of about $1 \times$

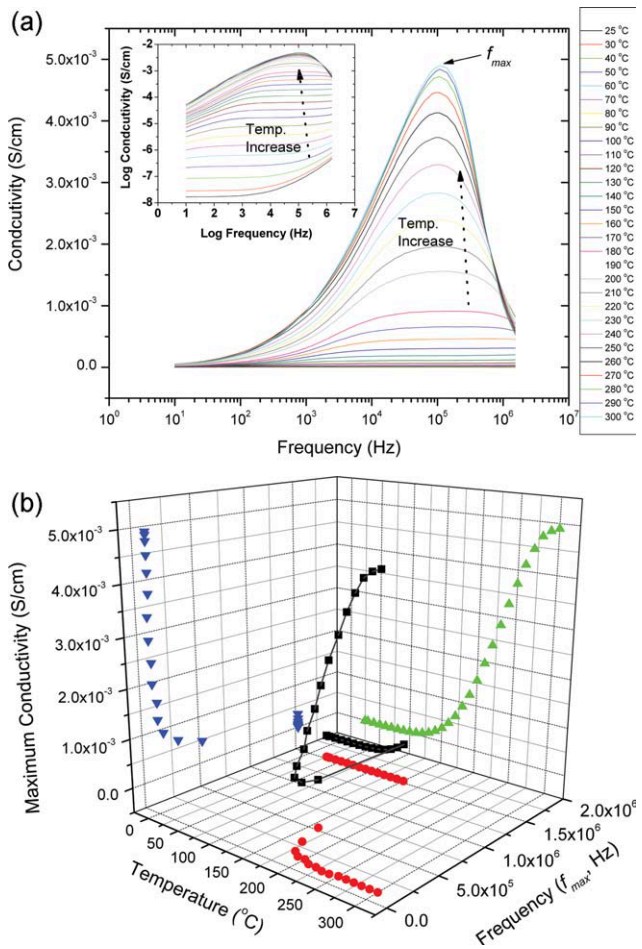

Figure 5 (a) Conductivity of PBI doped with 50 wt % of H_3PO_4 aqueous solution as functions of frequency and temperature and (b) 3D plot of maximum conductivity, temperature, and frequency. [Color figure can be viewed in the online issue, which is available at wileyonlinelibrary.com.]

10^5 Hz. This is fairly close to the frequency at which the dielectric constant reached its most negative value.

Figure 5(b) shows a similar relationship and a clear transition among the conductivity, temperature, and frequency to the dielectric constant as shown in Figure 4(b). The maximum conductivity as a function of f_{max} frequency was recorded at each temperature and plotted in a 3D space [shown as black solid squares in Fig. 5(b)]. From the projected data on the conductivity-temperature plane (green triangles in the graph), it is shown that the maximum conductivity slightly increased over the temperature range of 25–120°C. At 130 ± 0.1°C, the maximum conductivity began to decrease gradually, and above 160 ± 0.1°C, it increased steeply and reached 4.90×10^{-3} S/cm at 300 ± 0.1°C, showing a plateau. The projected data on the frequency-temperature plane (red circles in the graph) clarifies the relationship between the f_{max} frequency at the maximum conductivity and the temperature. The discontinuous transition is seen at 160 ± 0.1°C. Below 150 ± 0.1°C, the frequency (f_{max}) of maximum conductivity is insensitive to increasing temperature. Above 160 ± 0.1°C, however, the frequency (f_{max}) of maximum conductivities drops dramatically, plateauing at about 1×10^5 Hz. The similar big transition is evident in the data projection on the conductivity-frequency plane (blue inversed triangles in the graph). Above 4×10^5 Hz, the maximum conductivity is relatively insensitive to the frequency. Below 4×10^5 Hz, however, the maximum conductivity increased dramatically with decreasing frequency over a very small frequency interval.

The temperature dependence of the conductivity is due to the mobility of ions in the doped PBI. Above 160 ± 0.1°C, the mobility of ions begins to increase because of the increased mobility of the chain segments of PBI at that temperature. The temperature dependence of the dielectric and conductivity data suggests that the glass transition temperature of the doped PBI is about 160 ± 0.1°C. This is consistent with the glass transition temperature of about 180°C measured by a DMA (Table I).

Based on the dielectric constant and the conductivity data, it can be assumed that the origin of negative dielectric constant with the resonance behavior is attributed to the mobile ions of the doped PBI at elevated temperatures. The effect of mobile ions on the dielectric constant can be caused by two mechanisms: a macroscopic induction effect and an ionic plasma resonance.

The macroscopic induction effect on the negative dielectric constant is known to exist in a composite comprised of conductive rod-fillers in a dielectric matrix. The dispersion of the effective dielectric constant can range from a relaxation type to a resonance one, depending on the conductivity and dimension of the inclusion.[14–16] It was reported that low conductivity inclusions influence the relaxation spectrum and high conductivity inclusions impact the resonance spectrum at a high frequency. Conductive thin rods interact with an external field like dipoles and a skin effect increases with increasing frequency.[14] This resonance spectrum can be explained as an inductor-capacitor (L-C) resonant circuit, because the internal surfaces of the metallic electrodes act as capacitor plates, and the dielectric medium (doped PBI) behaves like inductors.[27] These capacitor and inductor resonate when,

$$Z_C + Z_L = \frac{1}{i\omega C_1} + i\omega L \approx \frac{1}{i\omega C_1} + \frac{1}{i\omega C_2} = 0, \omega < \omega_p \quad (2)$$

where Z_C, and Z_L are the impedance of a capacitor and an inductor, respectively, L is inductance, ω_p is a plasma frequency, and the capacitance (C_1) is given in terms of the permittivity of free space, ε_0, the cross sectional area, A_1, and plate separation, d_1, by:

$$C_1 = \frac{\varepsilon_0 A_1}{d_1} \quad (3)$$

Thus, a capacitor (C_2) with a negative-dielectric (ε) filling appears to be an inductor and the circuit is resonant at a certain frequency ($C_2 = \varepsilon\varepsilon_0 A_2/d_2$, where A_2 and d_2 are the cross sectional area and plate separation, respectively). In our case, at temperatures below 160°C, the conductivity was not high enough, so the material displayed a dielectric relaxation spectrum. However, above 160 ± 0.1°C, the conductivity became so high that a resonance spectrum with a negative dielectric constant at kHz frequencies was observed. It is likely that the down-shift of the resonance frequency with an increase in temperature arose from the increase in conductivity.[14] The capacitor and inductor resonance of the dope PBI sample was demonstrated using a Colpitts oscillator circuit, where the doped PBI film sample acted as an inductor at the elevated temperature. Figure 6 shows oscillation response of doped PBI using a Colpitts oscillator. The Colpitts oscillator is an electronic oscillator circuit using the combination of an inductance (L) with a capacitance (C) for oscillation frequency determination [Fig. 6(a)].[28] A disk shaped PBI film (25.4 mm-diameter, 50 μm-thick) doped with 20 wt % H_3PO_4 was employed as an inductor. The doped PBI film was placed in a heater to monitor the change of oscillation behavior at elevated temperature up to 275°C under DC 3V operation voltage. The doped PBI film did not exhibit any oscillation response up to 150°C, and started showing oscillation above 175°C, indicating that the doped PBI film sample acted as an

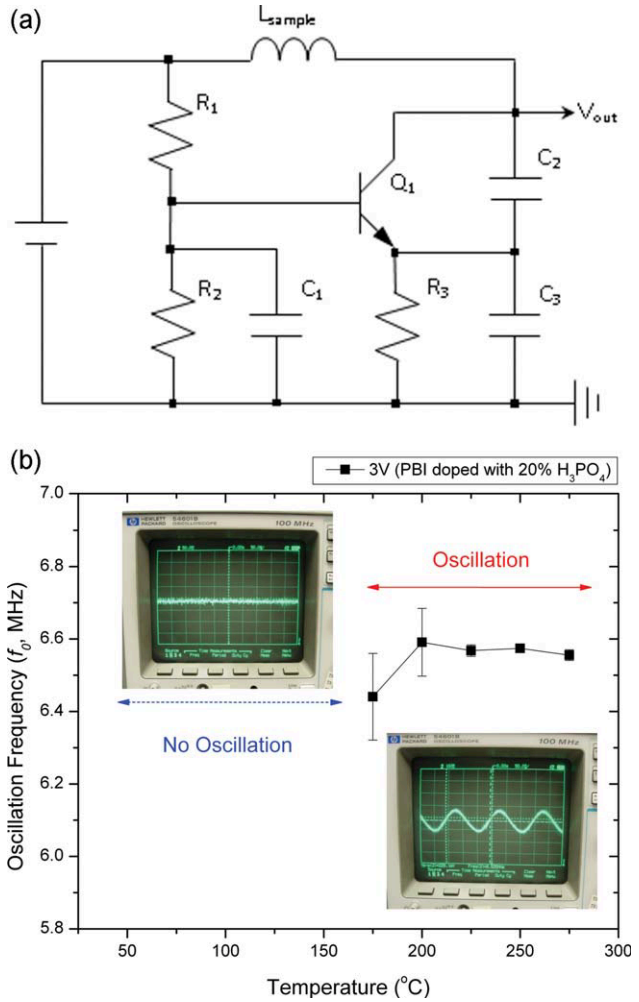

Figure 6 (a) Colpitts oscillator circuit (R_1: 10 kΩ; R_2: 10 kΩ; R_3: 10 kΩ; 2.2 kΩ; C_1: 0.01 μF; C_2: 561 pF; C_3: 561 pF; Q_1: 2N2222), and (b) Oscillation frequency of Colpitts oscillator installed with a doped PBI film as a function of temperature. [Color figure can be viewed in the online issue, which is available at wileyonlinelibrary.com.]

inductor at the elevated temperature. The oscillation frequency remained constant with increasing temperature within error range. In contrast, the Colpitts circuit did not oscillate up to 275°C in a short circuit void of doped PBI film inductor.

For the microscopic explanation of the negative dielectric behavior, the plasma frequency, ω_p of the doped PBI can be considered. Below the plasma frequency, ω_p, the dielectric constant is negative in the bulk of the conductive metal. For example, it is well known that the dielectric constant of aluminum is negative under its plasma frequency, ω_p of 15 eV (3.63×10^{15} Hz).[1] In our system, the charge carriers are not electrons as in aluminum but ions such as protons. The ion oscillation under an electric field appears at lower plasma frequency (ω_p^*) than a normal electron oscillation, given by $\omega_p^* = \omega_p \cdot (m_e/m_i)^{0.5}$.[29,30] Furthermore, both the interaction between electrons and ions and the lower density of charge can reduce the ion oscillation frequency.

Finally, an effect of the dopant concentration on the negative dielectric constant behavior was investigated. Figure 5(a,b) show the dielectric constant and the conductivity of PBI doped with 50 and 60 wt % phosphoric acid measured at 300 ± 0.1°C. In both cases, the dielectric constant increased with decreasing frequency at below resonance frequency. At low frequency, the dielectric constant of the PBI doped with 60 wt % phosphoric acid was higher than that of the PBI doped with 50 wt % phosphoric acid, which was expected because of higher concentration of mobile ions. In addition, the PBI doped with 60 wt % phosphoric acid showed a lower resonance

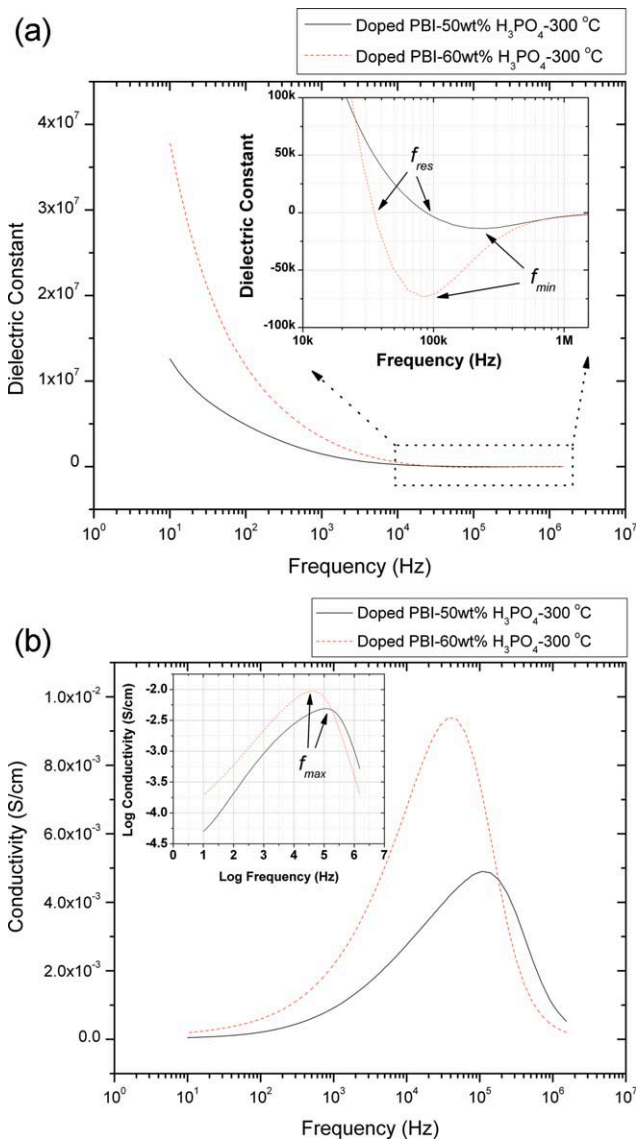

Figure 7 Comparison of (a) dielectric constant and (b) conductivity of PBI doped with different concentration of H_3PO_4 aqueous solution. [Color figure can be viewed in the online issue, which is available at wileyonlinelibrary.com.]

frequency, f_{res} and a more negative dielectric constant (ca. -7.35×10^4) at a lower frequency, f_{min} [inset of Fig. 7(a)]. Even at room temperature, the 60 wt % doped PBI showed a negative dielectric constant of -84.1 at 1.53×10^6 Hz. The 60 wt % doped PBI showed a higher peak (max) conductivity (ca. 9.4×10^{-3} S/cm) at a lower frequency, f_{max} (ca. 7.0×10^4 Hz) than the 50 wt % doped PBI [ca. 4.9×10^{-3} S/cm at 1.0×10^5 Hz, Fig. 7(b)], which is related to the more pronounced negative dielectric constant behavior. Highly doped PBI has sufficiently high conductivity to show a resonance behavior at lower temperature. It was found that the effect of increasing concentration of phosphoric acid was similar to that of increasing temperature on the negative dielectric constant because of higher mobility of ions as shown in Figure 4(a).

CONCLUSION

In summary, we have successfully developed a novel method to create a negative dielectric constant material, essential for making a NIM, by doping ions into a polymer, a protonated PBI. The PBI doped with phosphoric acid displays a negative dielectric constant at an elevated temperature due to a resonance behavior of mobile ions. The effective negative dielectric constant and the resonance frequency could be controlled by the concentration of the dopant. The capacitor and inductor resonance of the doped PBI sample was demonstrated at the elevated temperature using a Colpitts oscillator circuit to prove experimentally the role of the doped PBI film as an inductor. The doped PBI film sample acted as an inductor at the elevated temperature. This unique characteristic of doped PBI may be used to create homogenous negative dielectric constant materials with tunable resonance frequency and without complex geometric architectures consisting of capacitors and inductors or aggregated fillers.

The authors would like to thank Dr. Emilie Siochi, Dr. William T. Yost, and Dr. Godfrey Sauti for their valuable discussion and assistance. They would like the thank Mrs. Nancy Holloway and Mr. Vincent Cruz for their helps for sample preparation.

References

1. Pendry, J.; Holden, A.; Stewart, W.; Youngs, I. Phys Rev Lett 1996, 45, 4773.
2. Pendry, J.; Holden, D.; Sterwart, W. IEEE Trans Microwave Theory Tech 1999, 47, 2075.
3. Padilla, J.; Basov, D.; Smith, D. Mater Today 2006, 9, 28.
4. Pendry, J. B. Phys Rev Lett 2000, 85, 3966.
5. Shelby, R. A.; Smith, D. R.; Schultz, S. Science 2001, 292, 77.
6. Defense Sciences Office, Defense Advanced Research Projects Agency, Thrust Area, Materials, Novel Materials and Material Processes, Negative Index Materials Program. http://www.darpa.mil/dso/thrusts/materials/novelmat/nim/index.htm. Accessed January 11, 2008. Extract quotation taken from a previous DSO internet posting that is no longer accessible.
7. Schurig, D.; Mock, J. J.; Justice, B. J.; Cummer, S. A.; Pendry, J. B.; Starr, A. F. Smith, D. R. Science 2006, 314, 977.
8. Liu, H.; Liu, Y. M.; Li, T.; Wang, S. M., Zhu, S. N.; Zhang, X. Phys Status Solidi B 2009, 246, 1397.
9. Perrin, M.; Fasquel, S.; Decoopman, T.; Mélique, X.; Vanbésien, O.; Lheurette, E.; Lippens, D. J Opt A: Pure Appl Opt 2005, 7, S3.
10. Eleftheriades, G. V.; Iyer, A. K.; Kremer, P. C. IEEE Trans Microwave Theory Tech 2002, 50, 2702.
11. Grbic, A.; Eleftheriades, G. V. J Appl Phys 2002, 92, 5930.
12. Liu, L.; Caloz, C.; Chang, C.-C.; Itoh, T. J Appl Phys 2002, 92, 5560.
13. Marquès, R.; Martel, J.; Mesa, F.; Medina, F. Phys Rev Lett 2002, 89, 183901.
14. Lagarkov, A. N.; Matytsin, S. M.; Rozanov, K. N.; Sarychev A. K. J Appl Phys 1998, 84, 3806.
15. Markhnovskiy, D. P.; Panina, L. V. J Appl Phys 2003, 93, 4120.
16. Lagarkov, A. N.; Sarychev, A. K. Phys Rev B 1996, 53, 6318.
17. Padilia, W. J.; Smith, D. R.; Basov, D. N. J Opt Soc Am B 2006, 23, 404.
18. Institute of Physics. http://physicsworld.com/cws/article/news/2866. Accessed October 29, 2010.
19. Wang, J. T.; Wainwright, J. S.; Savinell, R. F. J Appl Electrochem 1996, 26, 751.
20. Pu, H. T.; Meyer, W. H.; Wegner, G. J Polym Sci Part B: Polym Phys 2002, 40, 663.
21. Pu, H. T.; Qiao, L.; Liu, Q.; Yang, Z. L. Eur Polym J 2005, 41, 2505.
22. Wolfe, J. F.; Sybert, P.D.; Sybert, J.R. U.S. Pat.4,5333,693 (1985).
23. Iwakura, Y.; Uno, K.; Imai, Y. J Polym Sci Part A: Gen Pap 1964, 2, 2605.
24. Bouchet, R.; Siebert, E. Solid State Ionics 1999, 118, 287.
25. Kawahara, M.; Morita, J.; Rikukawa, M.; Sannui, K.; Ogata, N. Electrochim Acta 2000, 45, 1395.
26. Ma, Y.; Wainwright, J. S.; Litt, M. H.; Savinell, R. F. J Electrochem Soc 2004, 151, A8.
27. Pendry, J. B. In Proc. NATO Advanced Study Inst. (Crete, NATO, ASI series); Soukoulis, C. M., Ed.; Dordrecht: Kluwer, 2001.
28. Colpitts, E. H. U.S. Pat.1,624,537 (1927).
29. Fried, B. D.; Gould, R. W. Phys Fluids 1961, 4, 139.
30. Harrison, E. R. Proc Phys Soc 1962, 80, 432.